Preparation and CO2 Sorption/Desorption of N-(3-Aminopropyl)Aminoethyl Tributylphosphonium Amino Acid Salt Ionic Liquids Supported into Porous Silica Particles

ARTICLE *in* INDUSTRIAL & ENGINEERING CHEMISTRY RESEARCH · MAY 2012

Impact Factor: 2.59 · DOI: 10.1021/ie2028415

3 AUTHORS, INCLUDING:

Linbo Wu
Zhejiang University
48 PUBLICATIONS **1,111** CITATIONS

SEE PROFILE

I&EC research
Industrial & Engineering Chemistry Research

Article

pubs.acs.org/IECR

Preparation and CO_2 Sorption/Desorption of *N*-(3-Aminopropyl) Aminoethyl Tributylphosphonium Amino Acid Salt Ionic Liquids Supported into Porous Silica Particles

Jie Ren, Linbo Wu,* and Bo-Geng Li

State Key Laboratory of Chemical Engineering at ZJU, Department of Chemical and Biological Engineering, Zhejiang University, Hangzhou 310027, China

Supporting Information

ABSTRACT: To search for robust CO_2 capture materials, several *N*-(3-aminopropyl)aminoethyl tributylphosphonium amino acid salts ([apaeP$_{444}$][AA])-type task specific ionic liquids (TSILs) were synthesized and immobilized into porous silica support through a facile impregnation−vaporization method. The ILs and thus prepared sorbents, Sorb-AA, were well characterized, and their CO_2 sorption and desorption behaviors under temperature- and vacuum-swing conditions were investigated. The ILs can be immobilized facilely into silica up to 1/1 IL/SiO_2 weight ratio. After IL loading, the sorbents retain reasonably high specific surface area and porosity and therefore exhibit rapid sorption and desorption rates as well as excellent sorption capacity and selectivity and can be used repeatedly. Among them, Sorb-Lys has the highest CO_2 sorption capacity. It can capture 1.54 mmol or 67.9 mg CO_2 per gram sorbent from a simulated flue gas containing 14% CO_2 in each cycle of sorption and desorption. Sorb-Gly has slightly less CO_2 sorption capacity, 1.37 mmol or 60.4 mg CO_2 per gram sorbent from the simulated flue gas, and much better long-term durability. It is estimated that it can retain 90% sorption capacity even after 1.38×10^3 cycles. These robust sorbents, especially Sorb-Gly, exhibit excellent potential in CO_2 capture applications.

1. INTRODUCTION

An increasing worldwide concern in global warming calls for more effective carbon capture and storage (CCS) technologies because emission of carbon dioxide (CO_2) plays a predominant role in global warming.[1] Capturing CO_2 from large emission sources like power plants using absorption or adsorption technology and storing it in geological formations has been proposed as a promising solution.[2] As a predominant commercialized approach for CO_2 capture, aqueous alkanolamine absorption technology is characterized by excellent sorption capacity and selectivity but also suffers from some inherent drawbacks including unavoidable absorbent loss, equipment corrosion, and high energy consumption during absorbent regeneration.[3] Therefore, new robust sorbent materials that can capture CO_2 more effectively and more economically have drawn greater attention from both academia and industry.

Ionic liquids (ILs) have been directly used or modified as CO_2 capture materials because they possess good CO_2 solubility or absorption capacity as well as low volatility, good thermal stability, and tunable properties.[4−9] Since Blanchard et al. first reported the solubility of CO_2 in imidazolium-based ILs,[10] a lot of research concerning the absorption mechanism have been reported.[11−14] Due to the physical absorption mechanism, the originally investigated ILs like [hmim][PF_6][15] only yield CO_2 solubility less than 0.088 wt % (exposed to CO_2 at 1 atm) which is not sufficient for practical CO_2 capture.[16−21] Taking a cue from the chemistry of aqueous organic amines, Bates et al. synthesized the first so-called task-specific ionic liquid (TSIL) in 2002. The TSIL has an amino group tethered to its imidazolium cation and possesses an absorption capacity of 0.5 mol CO_2/mol IL, which is in accordance with the theoretical value according to a 1:2 chemical absorption mechanism akin to that observed for aqueous amines.[15] Subsequently, a number of research groups have explored other amine-functionalized ILs to improve CO_2 absorption capacity. Among them, phosphonium amino acid salt ILs containing amino groups in anions ([P_{4444}][AA]-type)[22] or in both anions and cations ([aP_{4443}][AA]-type, dual amino-functionalized ILs)[23] exhibit good CO_2 absorption capacity as well as better thermal stability than the imidazolium counterparts.[24] Moreover, it is beneficial to reduce the cost of ILs by employing certain inexpensive amino acids such as glycine instead of fluorine-containing precursors. Wang et al. reported novel superbase-derived protic ILs that exhibit equimolar CO_2 absorption but poor thermal stability.[25] Very recently, they developed a class of more stable phosphonium ILs with weak proton donors as anions which possessed desirable enthalpy of CO_2 absorption and high absorption capacity.[26]

On the other hand, direct use of IL in CO_2 absorption often suffers from low sorption and desorption rate because of troublesome hyperviscosity of ILs.[27] Less viscous TSILs have been explored,[28,29] but their thermal stability is often not satisfactory. Tang et al. prepared a series of imidazolium-based poly(ionic liquid)s and found such polymer powders possessed much higher sorption rate and improved sorption capacity than the starting ILs, but the physical sorption capacity is still not high enough.[30−35] However, immobilization of TSILs into porous inorganic supports[22] not only significantly enhances the

Received: December 5, 2011
Revised: May 14, 2012
Accepted: May 16, 2012
Published: May 16, 2012

dx.doi.org/10.1021/ie2028415 | *Ind. Eng. Chem. Res.* 2012, 51, 7901−7909

Scheme 1. Schematic Diagram of Synthesis and Immobilization of Multiamino Functionalized TSILs [apaeP$_{444}$][AA][a]

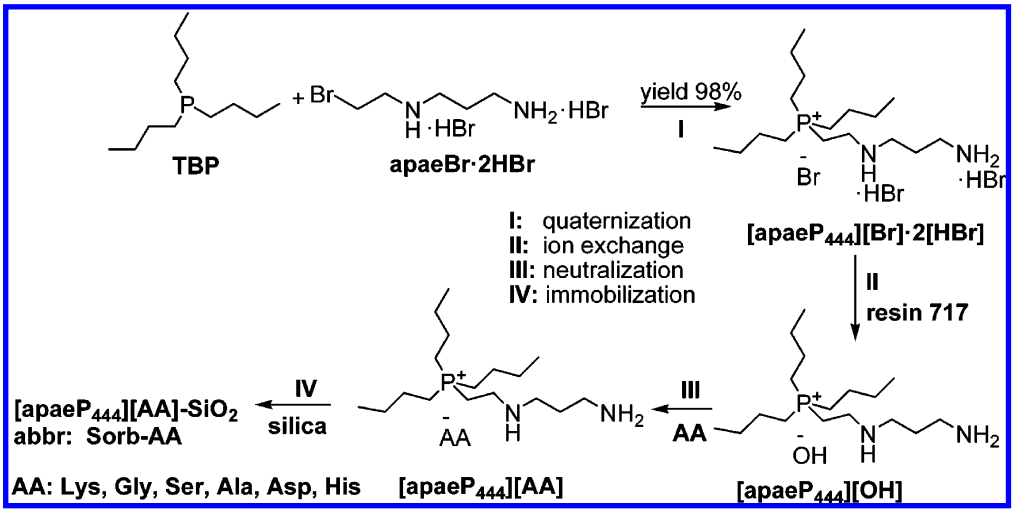

[a]Six amino acids (AA) were used: L-lysine (Lys), glycine (Gly), serine (Ser), alanine (Ala), aspartic acid (Asp), and histidine (His).

CO_2 sorption rate, because the specific surface area of TSILs and consequently the mass transfer in TSILs is significantly intensified after immobilization, but also keeps the high CO_2 sorption capacity of the TSILs themselves. Such strategy has also been utilized in the capture of SO_2.[36] Although there are usually some challenges such as poor heat recovery and less sorption capacity associated with typical solid sorbents, such new solid sorbents can combine the advantages of both liquid absorbent and solid adsorbent.[37,38] Therefore, immobilizing new TSILs on porous solid support is believed to be a promising strategy to prepare robust adsorbent for CO_2 capture.

Aiming to obtain new robust materials for CO_2 capture, we synthesized *N*-(3-aminopropyl)aminoethyl tributylphosphonium amino acid salts ([apaeP$_{444}$][AA]), well-designed TSILs with two amino groups in the cation and one or two in the anions, and immobilized them into porous silica through a facile impregnation−vaporization method. The TSILs and thus prepared sorbents were well characterized; their CO_2 sorption and desorption behaviors were investigated in detail, and the sorption mechanism involved was also discussed. The sorbents exhibit high sorption rate and capacity, excellent selectivity, good recyclability, high thermal stability, and long-term durability.

2. EXPERIMENTAL PART

2.1. Materials. Tri-*n*-butylphosphine (TBP, ≥98.5%, Shanghai Chuanhai Chem. Co., China), *N*-(2-bromoethyl)-1,3-propanediamine dihydrobromide (apaeBr·2HBr, ≥99%, Beijing Lumei Xinyue Biotechnology Centre, China), six amino acids (L-lysine (Lys), glycine (Gly), serine (Ser), alanine (Ala), aspartic acid (Asp), histidine (His), ≥99%, Shanghai Feiya Sci. & Tech. Co., Ltd., China) and porous silica (SiO_2, SI 1700, Grace Co., USA) were all used as received. Anion-exchange resin-717 (Cl-type, Shuanglin Chem. Reagent Plant, Hangzhou, China) was pretreated to become OH-type before use by a standard procedure.[22] Carbon dioxide (CO_2, ≥99.995%) and nitrogen (N_2, ≥99.5%) were purchased from Hangzhou Jingong Special Gas Co., Ltd., China, and used as received. Ethanol, acetonitrile, and *n*-hexane were all of analytical reagents and purchased from the National Medicine Co., China.

2.2. Synthesis of [apaeP$_{444}$][AA]. The [apaeP$_{444}$][AA] ionic liquids were synthesized via a three-step process: quaternization, ion exchange, and neutralization, as illustrated in Scheme 1.

N-(3-Aminopropyl)aminoethyl tributylphosphonium bromide dihydrobromide ([apaeP$_{444}$][Br]·2[HBr]) was synthesized via a typical quaternization method previously reported.[23] In brief, a mixture of TBP (42.5 g, 0.21 mol) and apaeBr·2HBr (68.6 g, 0.2 mol) in acetonitrile (150 mL) was reacted at 80 °C under N_2 atmosphere in a three-neck flask equipped with a reflux condenser and mechanical stirrer. After reflux for 24 h, the acetonitrile was distilled under vacuum at 70 °C and the residue was dried under vacuum at 80 °C for 24 h. The solid product was washed with hexane (100 mL) repeatedly under reflux, until there was no TBP detected in the distillation of the upper hexane phase. The product was further dried at 80 °C under vacuum for 24 h, and a light yellow solid, [apaeP$_{444}$]-[Br]·2[HBr], was obtained in good yield (98%, 107.2 g, 0.197 mol).

[apaeP$_{444}$][Br]·2[HBr] was dissolved in deionized water to prepare an aqueous solution (2 M) and passed through a pretreated anion exchange resin-717 (OH-type) column (L = 100 cm, d = 3 cm). Chloride-free *N*-(3-aminopropyl)-aminoethyl tributylphosphonium hydroxide ([apaeP$_{444}$][OH]) solution was collected and then concentrated through rotation evaporation at a temperature below 50 °C because pure [apaeP$_{444}$][OH] was not stable and would decompose above 50 °C.[39]

Then, the [apaeP$_{444}$][OH] solution was neutralized with a slight excess of an amino acid solution while stirring at room temperature for 12 h. After evaporation of water and then drying at 80 °C under vacuum for 24 h, a crude product containing the desired IL and unreacted amino acid was obtained. Ethanol was added into the crude product, and the mixture was vigorously agitated and then centrifuged at 8000 rpm for 15 min to remove the insoluble amino acid. The ethanol in the resultant solution was removed by rotating evaporation. After drying at 80 °C under vacuum for 24 h, [apaeP$_{444}$][AA] IL was finally obtained in an overall yield of 70−77%.

2.3. Immobilization of [apaeP$_{444}$][AA]. Immobilization of [apaeP$_{444}$][AA] into porous silica support was carried out with

dx.doi.org/10.1021/ie2028415 | Ind. Eng. Chem. Res. 2012, 51, 7901−7909

the aid of ethanol solvent according to our previously reported impregnation−vaporization method.[36] For simplicity, the resulting sorbent, or immobilized IL, was denoted as Sorb-AA(x/y), in which x/y is the weight ratio of the immobilized IL to the silica support. The ratio was controlled in the range from 0.5/1 to 1.5/1 by adjusting the feed ratio. The prepared sorbents were stored in a desiccator before use.

2.4. Characterization. The ionic liquids were characterized by ^{1}H NMR, ^{13}C NMR (Bruker Advance 2B, 400 MHz, D_2O), elemental analysis (Flash EA1112, ThermoFinnigan Co.), and FTIR (Nicolet 5700) to determine their chemical structures. FTIR was also used to compare the difference between blank and CO_2-saturated Sorb-AA samples. For the FTIR measurement of IL, an ethanol solution was used. For sorbents, a disk made of the sorbent and KBr was used.

Differential scanning calorimetry (DSC, Perkin-Elmer DSC-7) was conducted to measure melting temperature (T_m) of the TSILs. Thermogravimetric analysis (TGA) of [apaeP$_{444}$][AA] and Sorb-AA was performed on a Perkin-Elmer Instrument Pyris 1 TGA under N_2 atmosphere with a heating rate of 20 °C/min.

The pore size distribution, specific surface area, and porosities of SiO_2 and Sorb-AA were characterized with a mercury intrusion method (PoreMaster-60, Quantachrome Co.). In a standard procedure, about 1.5 g of fully dried sample was weighed and charged into a chamber. The chamber was then evacuated, and mercury was introduced to surround the sample. Then, programmed external pressure was applied and gradually increased up to 400 MPa, so the mercury penetrated into the pores under the external pressure. A series of pressures and corresponding intruded volumes provided the basic information for pore size distribution calculations. Pore size from 0.003 to 400 μm could be assessed in principle.

2.5. CO_2 Sorption and Desorption. For the sorbents and [apaeP$_{444}$][Gly] (which is a solid at room temperature), the sorption/desorption experiments were carried out in a U-tube. The apparatus and method were the same as previously described.[36,40,41] For [apaeP$_{444}$][Lys], which is liquid but has troublesomely high viscosity, the experiments were conducted in a strains bottle with or without stirring in order to investigate the effect of the diffusion of CO_2 in the IL. The sorption was carried out at 25 °C under atmospheric pressure with a gas flow rate of 50 mL/min unless otherwise specified, and desorption was performed at 90 °C under 8 kPa. Pure CO_2 gas was used in all the sorption experiments unless otherwise specified. In some cases, N_2 + CO_2 mixed gas containing 14% CO_2 was used as simulated flue gas. Repeated experiments gave an estimate of the experimental error at a level of ±5%.

3. RESULTS AND DISCUSSION

3.1. Characterization and Immobilization of [apaeP$_{444}$][AA] ILs. Considering the amino group(s) in a TSIL is(are) the true active site(s) for CO_2 sorption,[15,22,23,28,29,42,43] six *N*-(3-aminopropyl)aminoethyl tributylphosphonium amino acid salts ([apaeP$_{444}$][AA]) were synthesized. These TSILs contain 3−4 amino groups, i.e., two amino groups (one —NH and one —NH_2) in cations and one or two —NH_2 group(s) in anions, so 1.5−2.0 mol CO_2 can be captured by one mol IL theoretically according to the 1:2 (CO_2:amino) stoichiometry.[15]

Among the six ILs, [apaeP$_{444}$][Gly] and [apaeP$_{444}$][Ala] appear to be wax-like solid (T_m of 144 and 35 °C, respectively, by DSC) and others are liquid at room temperature, see Figure 1. The difference in condensed state may result from the difference in anion volume and in Coulombic and hydrogen bond interactions between the ion pair. As the ILs are very hygroscopic, [apaeP$_{444}$][Gly] and [apaeP$_{444}$][Ala] are prone to liquidize after absorbing a little amount of water.

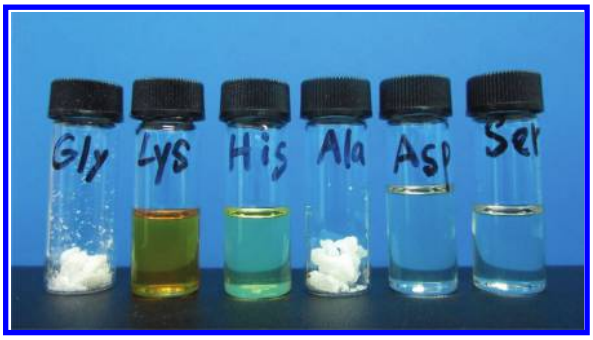

Figure 1. Appearances of six [apaeP$_{444}$][AA] ionic liquids. From left to right: [apaeP$_{444}$][Gly], [apaeP$_{444}$][Lys], [apaeP$_{444}$][His], [apaeP$_{444}$]-[Ala], [apaeP$_{444}$][Asp], and [apaeP$_{444}$][Ser].

The ^{1}H NMR, ^{13}C NMR, and FTIR spectra and elemental analysis data validated the expected structures of the six ILs, see Supporting Information. All the ILs have an onset thermal decomposition temperature (T_d) above 200 °C (212−234 °C; see Table 1), suggesting reasonably good thermal stabilities.

Table 1. Physicochemical Properties of the Six [apaeP$_{444}$][AA] ILs

TSILs	M_w	yield (%)	appearance	T_m (°C)	T_d[b] (°C)
[apaeP$_{444}$][Lys]	448.67	70	liquid, yellow, transparent	nd	234
[apaeP$_{444}$][Gly]	377.55	77	solid[a], white, wax-like	144	224
[apaeP$_{444}$][Ser]	407.57	58	liquid, colorless, transparent	nd	228
[apaeP$_{444}$][Ala]	391.57	72	solid[a], white, wax-like	35	212
[apaeP$_{444}$][Asp]	435.58	66	liquid, colorless, transparent	nd	212
[apaeP$_{444}$][His]	457.64	70	liquid, colorless, transparent	nd	226

[a]It is prone to liquidize and becomes a colorless, transparent liquid after absorbing a little amount of water. [b]Onset decomposition temperature is defined as the intersection of the initial baseline and the tangent of the weight−temperature curve as decomposition occurs.

The T_ds are comparable to or better than other ILs (80−281 °C, usually <200 °C) reported in the literature (see Supporting Information, Table S4). The T_ds of the ILs are lower than those of the corresponding amino acids.[44] This suggests that the thermal stability of the ILs is mainly determined by the [apaeP$_{444}$]$^+$ cation.

The ILs were immobilized into porous silica support using an impregnation−vaporization method[36] to prepare the CO_2 sorbents. The feed ratio of IL/SiO_2 ranged from 0.5/1 to 1.5/1 (w/w), and the actual IL/SiO_2 ratio in the sorbent was measured by TGA; see Figure 2. As shown in Table 2, the actual IL/SiO_2 ratio agrees well with the feed ratio when it is less than 1/1 but is lower than the feed ratio when it is above 1/1, presumably due to incomplete immobilization. Thus, prepared sorbents appear to be white powdery particles, like the

dx.doi.org/10.1021/ie2028415 | Ind. Eng. Chem. Res. 2012, 51, 7901−7909

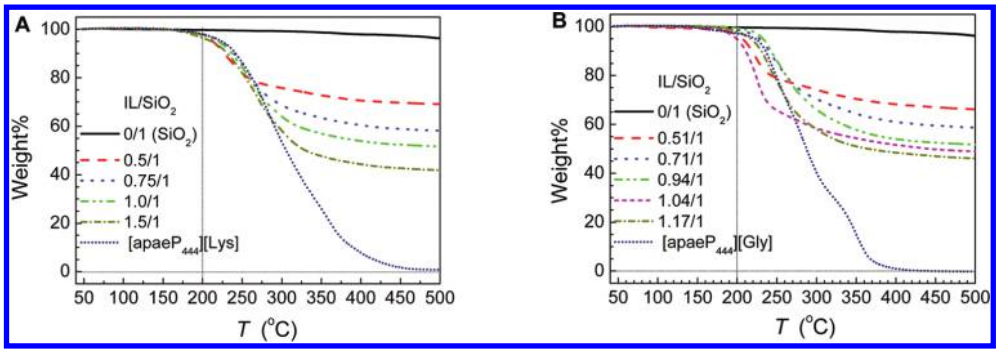

Figure 2. TGA curves of SiO_2, [apaeP$_{444}$][Lys], [apaeP$_{444}$][Gly], and the corresponding sorbents, Sorb-Lys and Sorb-Gly, with various IL/SiO_2 ratios (N_2 atmosphere, heating rate of 20 °C/min).

Table 2. Pore Characteristics[a] of SiO_2, Sorb-Lys, and Sorb-Gly Sorbents with Various IL/SiO_2 Ratios

	Sorb-Lys					Sorb-Gly				
IL/SiO_2[b]	IL/SiO_2[c]	V_p (cm^3/g)	A_p (m^2/g)	r_p (nm)	ϕ_{vp}	IL/SiO_2[c]	V_p (cm^3/g)	A_p (m^2/g)	r_p (nm)	ϕ_{vp}
0/1	0	3.36	414	16.3	85.7	0	3.36	414	16.3	85.7
0.5/1	0.45	2.04	150	27.2	75.7	0.51	1.96	137	28.6	75.2
0.75/1	0.72	1.64	80	40.9	70.5	0.71	1.55	95	32.8	69.6
1/1	0.94	1.22	42	58.9	64.1	0.94	1.21	58	42.0	63.3
1.25/1	/	/	/	/	/	1.04	0.99	31	63.5	57.7
1.5/1	1.39	0.87	11	163.6	54.9	1.17	0.86	19	91.5	53.8

[a] V_p, A_p, r_p, and ϕ_{vp} are total intrusion volume, specific surface area, average pore radius, and porosity, respectively. [b] IL/SiO_2 ratio in feed. [c] IL/SiO_2 in the sorbent.

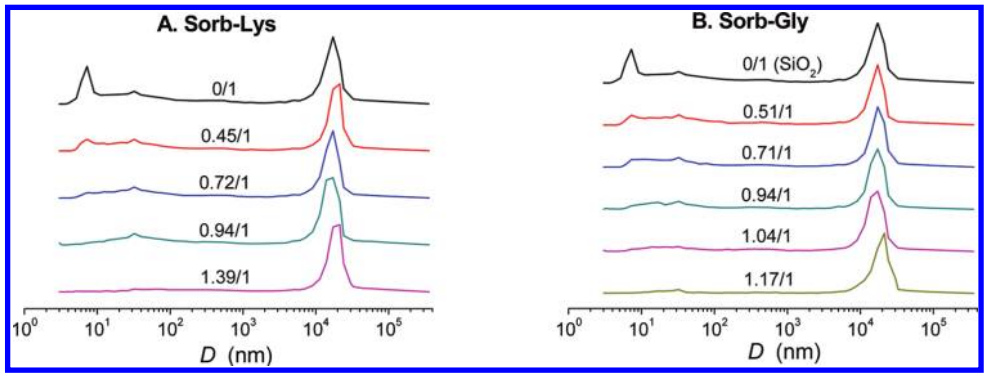

Figure 3. Pore size distributions of SiO_2, Sorb-Lys, and Sorb-Gly sorbents with various IL/SiO_2 ratios (Sorb-Lys: 0.45/1−1.39/1; Sorb-Gly: 0.51/1−1.17/1).

starting silica support, but the sorbent prepared at higher feed ratio of IL/SiO_2 (≥2) appeared to be wet and clay-like and was therefore neither characterized nor used for CO_2 sorption.

The thermal stability of the sorbents depends on the stability of the IL immobilized and is nearly independent of the IL loading, as seen in Figure 2. The T_ds are 100 °C higher than the desorption temperature (90 °C) used in this study.

The pore characteristics of blank silica support and the sorbents with various IL/SiO_2 ratios were characterized with a mercury intrusion method. The pore size distributions of Sorb-Lys and Sorb-Gly are illustrated in Figure 3, and the intrusion volume (V_p), specific surface area (A_p), porosity (ϕ_{vp}), and average pore radius (r_p) are summarized in Table 2. As expected, the V_p, A_p, and ϕ_{vp} all decrease with increasing IL loading. However, the r_p increases with increasing IL loading. This phenomenon is ascribed to the inner nanopores (3−100 nm) of silica support being first filled with IL and then gradually vanishing, leaving only micropores (~ 10^4 nm), as demonstrated in Figure 3. Similar pore characteristics were observed for other sorbents.[36] Anyhow, sufficient specific surface area and porosity are retained at IL/SiO_2 ratio around 1/1 owing to the retained micropores. These are very important for CO_2 sorption and desorption, as discussed below.

3.2. Basic CO_2 Sorption and Desorption Behaviors.

First, we investigated the CO_2 sorption behaviors of two typical ionic liquids, liquid [apaeP$_{444}$][Lys] and solid [apaeP$_{444}$][Gly], and the sorbents made from them, Sorb-Lys and Sorb-Gly. As illustrated in Figure 4, the sorption rate of solid [apaeP$_{444}$]-[Gly] was very slow and a clear "induction period" of about 60 min appeared before CO_2 sorption started. Its sorption capacity reached 0.66 mol CO_2/mol IL in 5 h. With comparison, the liquid [apaeP$_{444}$][Lys] (1.28 g, in a strains bottle without stirring) exhibited a much shorter "induction period" (10 min) and higher sorption rate (0.78 mol CO_2/mol IL in 3 h), but the sorption rate is still slow. The "induction period" of the ILs might result from non-Fickian diffusion.[45] During absorption, the ILs were gradually swollen by absorbed CO_2 and the

dx.doi.org/10.1021/ie2028415 | Ind. Eng. Chem. Res. 2012, 51, 7901−7909

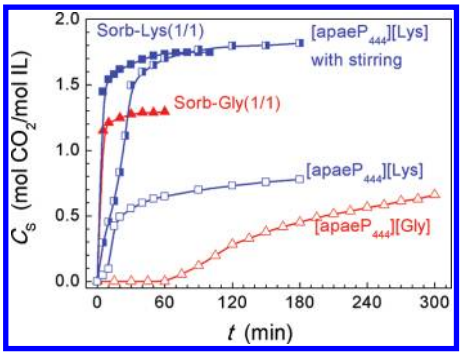

Figure 4. CO_2 sorption of $[apaeP_{444}][Gly]$ (△), $[apaeP_{444}][Lys]$ (□, 1.28 g, without stirring; ◨, 0.23 g, with vigorous stirring), Sorb-Gly(1/1) (▲), and Sorb-Lys(1/1) (■).

diffusion coefficient was raised accordingly. Therefore, the absorption accelerated after the "induction period".

When the amount of $[apaeP_{444}][Lys]$ was reduced to 0.23 g so that it could be effectively stirred with a magnetic stirrer, the sorption rate was significantly enhanced, reaching a sorption capacity of 1.82 mol CO_2/mol IL in 2 h, being close to the theoretical value, 2.0 mol CO_2/mol IL. However, it was found that the liquid $[apaeP_{444}][Lys]$ became white solid soon after CO_2 capture; see Figure 5. This will bring about inconvenience in practical application.

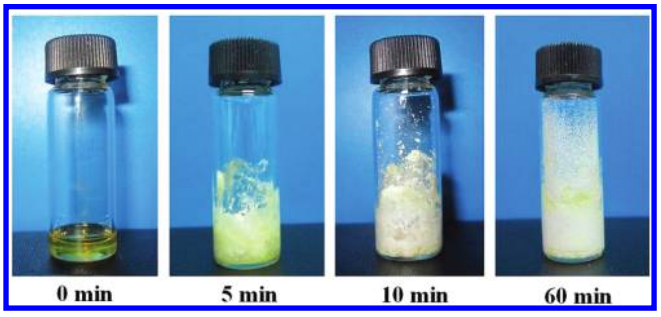

Figure 5. Solidification phenomenon of $[apaeP_{444}][Lys]$ during CO_2 capture.

In contrast, the two sorbents exhibit dramatically increased sorption rate when the mass transfer area of IL is enlarged after immobilization, and therefore, the mass transfer of CO_2 in IL is intensified.[22,36] The sorption capacity of Sorb-Gly reached 1.29 mol CO_2/mol IL in 1 h and that of $[apaeP_{444}][Lys]$ reached 1.73 mol CO_2/mol IL in 1 h. This method not only avoids the shortcoming mentioned above but also is applicable for RTIL as well as solid IL like $[apaeP_{444}][Gly]$.

The CO_2 sorption and desorption of the six sorbents prepared at IL/SiO_2 feed ratio of 1/1 are outlined in Figure 6, and the results are summarized in Table 3. All the sorbents exhibited rapid initial sorption rate and high capacity: 1−1.73 mol CO_2/mol IL. The CO_2 capture behaviors depend on the amino acid anion. Sorb-Lys exhibits highest sorption capacity, 1.73 mol CO_2/mol IL in 1 h (86% of its theoretical value), due to its highest content of amino, 4 amino groups in one molecule. The result is higher than those reported for other analogous ILs or immobilized ILs,[15,22,23,28,29,42,43,46,47] but it exhibits the slowest desorption rate. The other five sorbents almost reach their equilibrium sorption capacity in 1 h and exhibit different desorption rates. Among them, Sorb-Gly exhibits the best CO_2 capture performance: 1.29 mol CO_2/mol IL (86% of the theoretical value) in 1 h and rapid and complete desorption in 15 min.

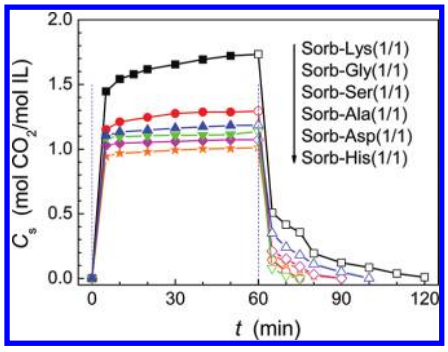

Figure 6. CO_2 sorption and desorption of six different sorbents prepared at IL/SiO_2 feed ratio of 1/1.

3.3. CO_2 Sorption Mechanism. The silica support itself has certain physical CO_2 adsorption ability (ca. 0.75 wt % or 0.17 mmol CO_2/g SiO_2), but its contribution to CO_2 capture reduces after IL immobilization because a majority of the surface is occupied by the IL. Thus, the CO_2 sorption capacity of the sorbents is mainly attributed to the sorption capacity of the immobilized ILs, as will be discussed later.

Figure 7 shows the FTIR spectra of Sorb-Lys before CO_2 sorption, after CO_2 sorption, and after CO_2 desorption. Before CO_2 sorption, the sorbent exhibits an absorption peak of the COO^- group in the $[Lys]^-$ anion around 1600 cm^{-1}. After CO_2 saturated, a new shoulder peak appeared at 1697 cm^{-1}, corresponding to the new formed carbamate on account of CO_2 chemical absorption. The absorption peak of —NH— bond is overlapped with that of hydroxyl on the surface of SiO_2 at 3300 cm^{-1}, so its change cannot be observed.[22] After CO_2 desorption, the shoulder peak at 1697 cm^{-1} disappears again and the spectrum agrees well with that before CO_2 sorption. The result suggests that the CO_2 captured could be completely desorbed, and the sorbents are suitable for reversible CO_2 capture. From the change in FTIR absorption and the rapid sorption rate, it can also be concluded that chemical absorption is predominant. Other sorption mechanisms like physical adsorption, absorption, and chemical adsorption are also involved, but their contributions to CO_2 capture are less important.[23]

It is well-known that aqueous amine captures CO_2 in a 1:2 (CO_2/amino) stoichiometry.[3] First, an amino group reacts with CO_2 to form a carbamic acid, and then the carbamic acid further reacts with another amino group to form carbamate and ammonium ion, as shown in Scheme 2.[42] For amino-functionalized TSILs, both 1:2[15] and 1:1[42,43] mechanisms have been proposed. Brennecke, Fuente, and their co-workers argued that the amino in anion follows 1:1 stoichiometry (only forming carbamic acid but not carbamate), while that in cation follows traditional 1:2 stoichiometry. The 1:1 stoichiometry agrees well with $[P_{66614}][AA]$-type ILs but not with other anion-functionalized ILs like $[N_{2222}][AA]$-type[28] and $[N_{2224}][AA]$-type.[29] It may not be the location of amino (anion vs cation) but the size of ion pair to determine the reaction mechanism. For ILs with large-sized ion pairs (like $[P_{66614}][AA]$), it is difficult for two amino groups to approach each other so that only carbamic acid is formed in 1:1 stoichiometry. For ILs (like $[N_{2222}][AA]$) with small ion pair size, the formed carbamic acid can approach and further react with another amino to form carbamate in 1:2 stiochiometry.

dx.doi.org/10.1021/ie2028415 | Ind. Eng. Chem. Res. 2012, 51, 7901−7909

Table 3. CO_2 Sorption Capacity (C_s) of the Six Sorbents Prepared at IL/SiO_2 Feed Ratio of 1/1

sample	number of amino	$C_{s,theo}$ (mol/mol)	$C_{s,exp}$ (mol/mol)[a]	$C_{s,exp}$ (mmol/g IL)	$C_{s,exp}$ (mmol/g sorb)
Sorb-Lys	4	2.0	1.73 (86%)	3.86	1.87
Sorb-Gly	3	1.5	1.29 (86%)	3.44	1.65
Sorb-Ser	3	1.5	1.19 (79%)	2.92	1.46
Sorb-Ala	3	1.5	1.14 (76%)	2.91	1.46
Sorb-Asp	3	1.5	1.07 (71%)	2.46	1.23
Sorb-His	3	1.5	1.01 (67%)	2.21	1.10

[a]Note: The data in parentheses are the percentages of experimental to theoretical CO_2 sorption capacities.

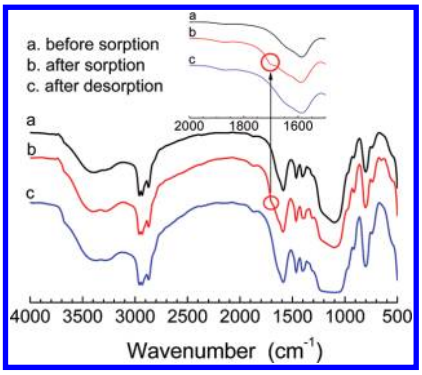

Figure 7. IR spectra of Sorb-Lys in CO_2 sorption/desorption process: (a) before sorption; (b) after CO_2 sorption; (c) after CO_2 desorption.

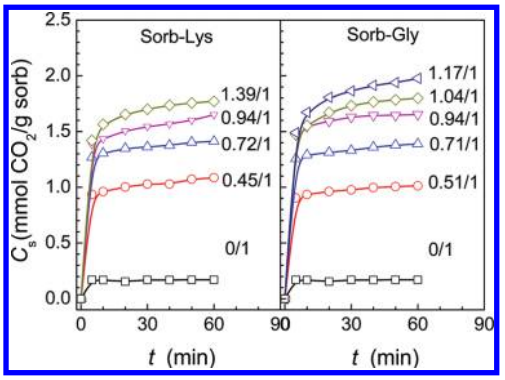

Figure 8. CO_2 sorption of blank SiO_2, Sorb-Lys, and Sorb-Gly with various IL/SiO_2 ratios.

Scheme 2. Reaction Schematics of CO_2 with Amino-Containing TSILs[42]

$$—NH_2 + CO_2 \rightleftharpoons —NHCOOH \quad (1)$$

$$—NHCOOH + —NH_2 \rightleftharpoons —NHCOO^- + —NH_3^+ \quad (2)$$

For ILs with intermediate ion pair size, both mechanisms exist. The assumption supports results previously reported in the literature.[22,23,28,29] In this study, the ion pair size of our [apaeP$_{444}$][AA]-type ILs approximates to that of [P$_{4444}$][AA]-type ILs,[22] so they tend to obey the 1:2 stoichiometry.

According to the 1:2 stiochiometry, 1.5−2.0 mol CO_2 can be captured per mol [apaeP$_{444}$][AA] IL at most. The experimental CO_2 sorption capacities are close to but still lower than the theoretical values; see Table 3. The reasons for the discrepancy may include: (1) The —NH— group tethered to the phosphonium cation may have less reactivity to react with CO_2 than the —NH_2 group. (2) Some amino groups form hydrogen bonds among themselves and therefore may become inactive for CO_2 sorption.[43]

3.4. Further Assessments for Practical Application. As Sorb-Lys and Sorb-Gly exhibit better CO_2 sorption capacity than other sorbents and Lys and Gly are less expensive amino acids, these two sorbents were further assessed in terms of effects of IL loading and water content, sorption/desorption cycles and long-term tolerance, and CO_2 capture behaviors for simulated flue gas.

As expected, higher IL loading led to higher CO_2 sorption capacity, as illustrated in Figure 8. With increasing the IL/SiO_2 ratio, it takes a longer time to reach the sorption equilibrium because the sorption rate slows down before reaching the equilibrium, but a high sorption value can still be reached in short time at high IL/SiO_2 ratio. When the CO_2 sorption capacity (C_s) was replotted with the weight fraction of IL in the sorbent ($\phi_{w,IL}$), it was found that the C_s exhibited an approximately linear increase with $\phi_{w,IL}$ in the experimental range; see Figure 9. This validates the predominant contribution of the immobilized IL to the C_s of the sorbent,

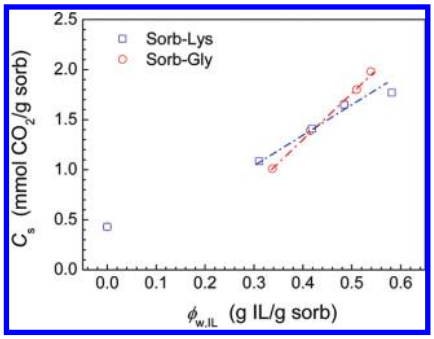

Figure 9. Dependence of CO_2 sorption capacity (C_s) of Sorb-Lys and Sorb-Gly on the weight fraction of IL in the sorbent, $\phi_{w,IL}$.

as discussed above. In this figure, the data point at $\phi_{w,IL}$ of zero is the sorption that results solely from the silica support. The contribution of the support on C_s reduces and changes with $\phi_{w,IL}$, so the straight lines do not pass through this data point.

Because the [apaeP$_{444}$][AA] ILs are hygroscopic and CO_2-containing flue gas often contains certain quantity of water vapor, the sorbent will absorb water vapor from and come into equilibrium with the flue gas. In the desorption step, the sorbent can be dried again. Therefore, the effect of water on CO_2 sorption should be considered. To estimate the possible maximum water content in the sorbents during adsorption, we measured the water sorption of sorbents at 25 °C (the same as adsorption temperature) in an airtight space in the presence of water. The results are shown in Supporting Information, Figure S4. The water content in both sorbents (Sorb-Gly and Sorb-Lys) increases with time to high values. It can be seen that the sorbents sorb 3 wt % water (based on the weight of the "wet" sorbent) in 2−3 h and 21 wt % water in 50 h. So, in a sorption

dx.doi.org/10.1021/ie2028415 | Ind. Eng. Chem. Res. 2012, 51, 7901−7909

process less than 2 h, the water content in the sorbent could be less than 3 wt %. Therefore, the CO_2 adsorption of the sorbents that absorbed 3 wt % water was studied. A sample absorbing much higher (21 wt %) water was also investigated for comparison. The results are shown in Figure 10.

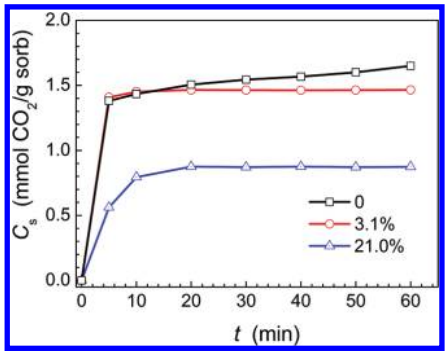

Figure 10. CO_2 sorption of Sorb-Lys (1/1) sorbents containing different amounts of water.

At a water content of 3.1%, the sorption capacity decreases by ~10% and the sorption rate is within error of that of the dry sample. At a water content of 21%, the sorption capacity decreases by ~50% and the sorption rate slows down clearly. Similar results also appeared in other reports.[36,48] The reason can be attributed to sorption competition between water and CO_2[36] and the hydrogen bond interaction between ILs and water.[49] In practical application, water absorbed in IL can be desorbed during desorption operation at high temperature and under vacuum, so the actual water content in a sorbent during the sorption process could be no more than 3%. This implies that the CO_2 sorption capacity only decreases slightly and the sorption rate remains unchanged.

The CO_2 sorption/desorption cycles are illustrated in Figure 11. Both sorbents can be used in cycles, keeping nearly constant

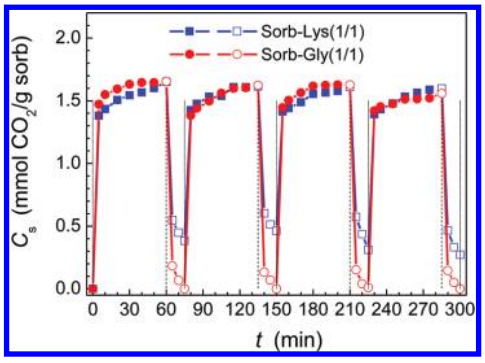

Figure 11. Adsorption/desorption cycles of Sorb-Lys (1/1) and Sorb-Gly(1/1).

sorption capacity. 5.7% and 3.1% loss in CO_2 sorption capacity were observed after four cycles for Sorb-Gly and Sorb-Lys, respectively. For Sorb-Gly, the sorption and desorption operations was completed in 60 and 15 min, respectively, and 1.65 mmol CO_2 was captured per gram sorbent in each cycle. Sorb-Lys has the same sorption capacity and rate, but its desorption was slower. As shown in Figure 12, its desorption was completed in 60 min.

The CO_2 sorption ability for CO_2/N_2 mixed gas was further assessed and compared with that for pure CO_2 and N_2. The

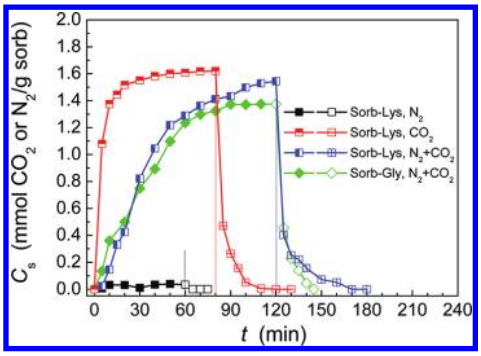

Figure 12. Sorption and desorption behaviors of the two sorbents (Sorb-Lys and Sorb-Gly) for pure CO_2, pure N_2, and their mixture.

CO_2 content in the mixture gas was set at 14% to simulate actual flue gas of coal-fired power plants.[3] The flow rates were 10 + 60 mL/min for the mixed gas, i.e., 10 and 60 mL/min for CO_2 and N_2, respectively. The results are visualized in Figure 12. The sorption capacity is excellent for pure CO_2 but negligible for pure N_2, indicating excellent sorption selectivity for CO_2. In comparison with pure CO_2, the sorption rate and capacity for simulated flue gas both decrease to a certain extent because of lower CO_2 concentration or partial pressure in the mixed gas. The sorption capacity reaches 1.54 and 1.37 mmol CO_2/g sorb in 120 min for Sorb-Lys (1/1) and Sorb-Gly(1/1), respectively, and the CO_2 captured is desorbed completely in 60 and 30 min, respectively.

To clarify the cause of the slight loss of sorption capacity shown in Figure 11, long-term durability of the sorbents were further assessed by keeping them under desorption condition (90 °C, 8.0 kPa). Ionic liquids have been reported to have certain volatility even usually possessing ultralow vapor pressure.[49−51] Figure 13 shows that the weight loss of the ILs

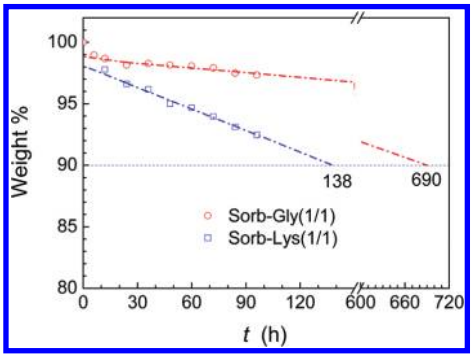

Figure 13. The weight loss of Sorb-Lys(1/1) and Sorb-Gly(1/1) with time under the desorption condition (90 °C, 8.0 kPa).

in the sorbents increased linearly with time (except the very beginning) and reached 15% and 7.4% in 96 h for Sorb-Lys and Sorb-Gly, respectively. It suggests that the slight loss of sorption capacity may result from weight loss of the immobilized IL under desorption conditions. The better stability of Sorb-Gly may be attributed to its less volatility and solid state at room temperature. From the linear regression, the two sorbents can retain 90% sorption capacity (i.e., 10% weight loss of IL) after desorption operation for 138 and 690 h. According to the desorption time (60 and 30 min) in separating CO_2 from simulated flue gas, it is estimated that Sorb-Lys and Sorb-Gly can endure 138 and 1.38×10^3 cycles, respectively, before their sorption capacity decreases by 10%. These results indicate that

dx.doi.org/10.1021/ie2028415 | Ind. Eng. Chem. Res. 2012, 51, 7901−7909

the sorbents have excellent long-term stability, especially the Sorb-Gly sorbent.

4. CONCLUSIONS

Six [apaeP$_{444}$][AA]-type ionic liquids were synthesized and immobilized into porous silica supports. The ILs and thus prepared sorbents, Sorb-AA, were well characterized, and their CO_2 sorption and desorption behaviors under temperature- and vacuum-swing conditions were investigated. The ILs exhibit good thermal stabilities up to 200 °C and can be facilely immobilized into silica up to 1/1 IL/SiO_2 weight ratio. After IL loading, the sorbents retain partial (depending on IL loading) pore characteristics of the support and the same thermal stability of the ILs. Therefore, they exhibit rapid sorption and desorption rates as well as excellent sorption capacity and selectivity and can be repeatedly recycled for CO_2 uptake. Among them, Sorb-Lys has the highest CO_2 sorption capacity. It can capture ca. 1.65 mmol or 72.6 mg CO_2 per gram sorbent from pure CO_2 and 1.54 mmol or 67.9 mg CO_2 per gram sorbent from a simulated flue gas containing 14% CO_2 in each cycle of sorption and desorption. Sorb-Gly has slightly less CO_2 sorption capacity, 1.37 mmol or 60.4 mg per gram sorbent from the simulated flue gas, but it has much better long-term durability. It is estimated that it can retain 90% sorption capacity after 1.38×10^3 cycles. By comparison, it is estimated that Sorb-Lys can endure 138 cycles. These results demonstrate the potential of these robust sorbents in CO_2 capture applications, especially for the Sorb-Gly sorbent.

■ ASSOCIATED CONTENT

Ⓢ Supporting Information

Details on the chemical structures, including ^{1}H NMR (Figure S1), ^{13}C NMR (Figure S2), FTIR (Figure S3) spectra and their attributions (Scheme S1, Tables S1-2), elemental analysis data (Table S3) of the six ILs and their intermediate, [apaeP444]-[Br]·2[HBr], and a table (Table S4) on comparison of the decomposition temperatures of various amino acid ILs in this study and those reported in literature and a figure (Figure S4) on water sorption of two sorbents. This material is available free of charge via the Internet at http://pubs.acs.org.

■ AUTHOR INFORMATION

Corresponding Author

*E-mail: wulinbo@zju.edu.cn.

Notes

The authors declare no competing financial interest.

■ ACKNOWLEDGMENTS

The authors thank the National High Technology Research and Development Program of China (863 Program, 2008AA062302) and the Natural science foundation of Zhejiang Province (Y404084, Y407038) and PCSIRT for financial support.

■ REFERENCES

(1) Hunt, A. J.; Sin, E. H. K.; Marriott, R.; Clark, J. H. Generation, capture, and utilization of industrial carbon dioxide. *ChemSusChem* **2010**, *3*, 306.

(2) Yu, K. M. K.; Curcic, I.; Gabriel, J.; Tsang, S. C. E. Recent advances in CO_2 capture and utilization. *ChemSusChem* **2008**, *1*, 893.

(3) Rochelle, G. T. Amine scrubbing for CO_2 capture. *Science* **2009**, *325*, 1652.

(4) Bara, J. E.; Carlisle, T. K.; Gabriel, C. J.; Camper, D.; Finotello, A.; Gin, D. L.; Noble, R. D. Guide to CO_2 separation in imidazolium-based room-temperature ionic liquids. *Ind. Eng. Chem. Res.* **2009**, *28*, 2739.

(5) Hasib-ur-Rahman, M.; Siaj, M.; Larachi, F. Ionic liquids for CO_2 capture-development and progress. *Chem. Eng. Process.* **2010**, *49*, 313.

(6) Han, D.; Row, K. H. Recent applications of ionic liquids in separation technology. *Molecules* **2010**, *15*, 2405.

(7) Wappel, D.; Gronald, G.; Kalb, R.; Draxler, J. Ionic liquids for post-combustion CO_2 absorption. *Int. J. Greenhouse Gas Control* **2010**, *4*, 486.

(8) Karadas, F.; Atilhan, M.; Aparicio, S. Review on the use of ionic liquids (ILs) as alternative fluids for CO_2 capture and natural gas sweetening. *Energy Fuels* **2010**, *24*, 5817.

(9) Bara, J. E.; Camper, D.; Gin, D. L.; Noble, R. D. Room-temperature ionic liquids and composite materials: Platform technologies for CO_2 capture. *Acc. Chem. Res.* **2010**, *43*, 152.

(10) Blanchard, L. A.; Hancu, D.; Beckman, E. J.; Brennecke, J. F. Green processing using ionic liquids and CO_2. *Nature* **1999**, *399*, 28.

(11) Cadena, C.; Anthony, J. L.; Shah, J. K.; Morrow, T. I.; Brennecke, J. F.; Maginn, E. J. Why is CO_2 so soluble in imidazolium-based ionic liquids? *J. Am. Chem. Soc.* **2004**, *126*, 5300.

(12) Scovazzo, P.; Camper, D.; Kieft, J.; Poshusta, J.; Koval, C.; Noble, R. D. Regular solution theory and CO_2 gas solubility in room-temperature ionic liquids. *Ind. Eng. Chem. Res.* **2004**, *43*, 6855.

(13) Maiti, A. Theoretical screening of ionic liquid solvents for carbon capture. *ChemSusChem* **2009**, *2*, 628.

(14) Huang, J.; Rüther, T. Why are ionic liquids attractive for CO_2 absorption? An overview. *Aust. J. Chem.* **2009**, *62*, 298.

(15) Bates, E. D.; Mayton, R. D.; Ntai, I.; Davis, J. H. CO_2 capture by a task-specific ionic liquid. *J. Am. Chem. Soc.* **2002**, *124*, 926.

(16) Scovazzo, P.; Camper, D.; Kieft, J.; Poshusta, J.; Koval, C.; Noble, R. D. Regular solution theory and CO_2 gas solubility in room-temperature ionic liquids. *Ind. Eng. Chem. Res.* **2004**, *43*, 6855.

(17) Shiflett, M. B.; Yokozeki, A. Solubilities and diffusivities of carbon dioxide in ionic liquids: [bmim][PF_6] and [bmim][BF_4]. *Ind. Eng. Chem. Res.* **2005**, *44*, 4453.

(18) Shiflett, M. B.; Yokozeki, A. Solubility of CO_2 in room temperature ionic liquid [hmim][Tf_2N]. *J. Phys. Chem. B* **2007**, *111*, 2070.

(19) Finotello, A.; Bara, J. E.; Camper, D.; Noble, R. D. Room-temperature ionic liquids: Temperature dependence of gas solubility selectivity. *Ind. Eng. Chem. Res.* **2008**, *47*, 3453.

(20) Carlisle, T. K.; Bara, J. E.; Gabriel, C. J.; Noble, R. D.; Gin, D. L. Interpretation of CO_2 solubility and selectivity in nitrile-functionalized room-temperature ionic liquids using a group contribution approach. *Ind. Eng. Chem. Res.* **2008**, *47*, 7005.

(21) Revelli, A. L.; Mutelet, F.; Jaubert, J. N. High carbon dioxide solubilities in imidazolium-based ionic liquids and in poly(ethylene glycol) dimethyl ether. *J. Phys. Chem. B* **2010**, *114*, 12908.

(22) Zhang, J. M.; Zhang, S. J.; Dong, K.; Zhang, Y. Q.; Shen, Y. Q.; Lv, X. M. Supported absorption of CO_2 by tetrabutylphosphonium amino acid ionic liquids. *Chem.—Eur. J.* **2006**, *12*, 4021.

(23) Zhang, Y. Q.; Zhang, S. J.; Lu, X. M.; Zhou, Q.; Fan, W.; Zhang, X. P. Dual amino-functionalised phosphonium ionic liquids for CO_2 capture. *Chem.—Eur. J.* **2009**, *15*, 3003.

(24) Fukumoto, K.; Yoshizawa, M.; Ohno, H. Room temperature ionic liquids from 20 natural amino acids. *J. Am. Chem. Soc.* **2005**, *127*, 2398.

(25) Wang, C. M.; Luo, H. M.; Jiang, D. E.; Li, H. R.; Dai, S. Carbon dioxide capture by superbase-derived protic ionic liquids. *Angew. Chem., Int. Ed.* **2010**, *49*, 5978.

(26) Wang, C. M.; Luo, X. Y.; Luo, H. M.; Jiang, D. E.; Li, H. R.; Dai, S. Tuning the basicity of ionic liquids for equimolar CO_2 capture. *Angew. Chem., Int. Ed.* **2010**, *50*, 4918.

(27) Gutowski, K. E.; Maginn, E. J. Amine-functionalized task-specific ionic liquids: A mechanistic explanation for the dramatic increase in viscosity upon complexation with CO_2 from molecular simulation. *J. Am. Chem. Soc.* **2008**, *130*, 14690.

(28) Jiang, Y. Y.; Wang, G. N.; Zhou, Z.; Wu, Y. T.; Geng, J.; Zhang, Z. B. Tetraalkylammonium amino acids as functionalized ionic liquids of low viscosity. *Chem. Commun.* **2008**, 505.
(29) Yu, H.; Wu, Y. T.; Jiang, Y. Y.; Zhou, Z.; Zhang, Z. B. Low viscosity amino acid ionic liquids with asymmetric tetraalkylammonium cations for fast absorption of CO_2. *New J. Chem.* **2009**, *33*, 2385.
(30) Tang, J.; Sun, W.; Tang, H.; Radosz, M.; Shen, Y. Enhanced CO_2 absorption of poly(ionic liquid)s. *Macromolecules* **2005**, *38*, 2037.
(31) Tang, J.; Tang, H.; Sun, W.; Radosz, M.; Shen, Y. Poly(ionic liquid)s as new materials for CO_2 absorption. *J. Polym. Sci., A: Polym. Chem.* **2005**, *43*, 5477.
(32) Tang, J.; Tang, H.; Sun, W.; Radosz, M.; Shen, Y. Low-pressure CO_2 sorption in ammonium-based poly(ionic liquid)s. *Polymer* **2005**, *46*, 12460.
(33) Blasig, A.; Tang, J.; Hu, X.; Tan, S.; Shen, Y.; Radosz, M. Carbon dioxide solubility in polymerized ionic liquids containing ammonium and imidazolium cations from magnetic suspension balance: P[VBTMA][BF_4] and P[VBMI][BF_4]. *Ind. Eng. Chem. Res.* **2007**, *46*, 5542.
(34) Tang, J.; Shen, Y.; Radosz, M.; Sun, W. Isothermal carbon dioxide sorption in poly(ionic liquid)s. *Ind. Eng. Chem. Res.* **2009**, *48*, 9113.
(35) Zhao, Q. C.; Wajert, J. C.; Anderson., J. L. Polymeric ionic liquids as CO_2 selective sorbent coatings for solid-phase microextraction. *Anal. Chem.* **2010**, *82*, 707.
(36) Zhang, Z. M.; Wu, L. B.; Dong, J.; Li, B. G.; Zhu, S. P. Preparation and SO_2 sorption/desorption behavior of an ionic liquid supported on porous silica particles. *Ind. Eng. Chem. Res.* **2009**, *48*, 2142.
(37) Liu, S. H.; Wu, C. H.; Lee, H. K.; Liu, S. B. Highly stable amine-modified mesoporous silica materials for efficient CO_2 capture. *Top. Catal.* **2010**, *53*, 210.
(38) Goeppert, A.; Czaun, M.; May, R. B.; Prakash, G. K. S.; Olah, G. A. Carbon dioxide capture from the air using a polyamine based regenerable solid adsorbent. *J. Am. Chem. Soc.* **2011**, *133*, 20164.
(39) Kagimoto, J.; Fukumoto, K.; Ohno, H. Effect of tetrabutylphosphonium cation on the physico-chemical properties of amino-acid ionic liquids. *Chem. Commun.* **2006**, *21*, 2254.
(40) Wu, L. B.; An, D.; Dong, J.; Zhang, Z. M.; Li, B. G.; Zhu, S. P. Preparation and SO_2 absorption/desorption properties of crosslinked poly(1,1,3,3-tetramethylguanidinium acrylate) porous particles. *Macromol. Rapid Commun.* **2006**, *27*, 1949.
(41) An, D.; Wu, L. B.; Li, B. G.; Zhu, S. P. Synthesis and SO_2 absorption/desorption properties of poly(1,1,3,3-tetramethylguanidinium acrylate). *Macromolecules* **2007**, *40*, 3388.
(42) Gurkan, B. E.; de la Fuente, J. C.; Mindrup, E. M.; Ficke, L. E.; Goodrich, B. F.; Price, E. A.; Schneider, W. F.; Brennecke, J. F. Equimolar CO_2 absorption by amine-functionalized ionic liquids. *J. Am. Chem. Soc.* **2010**, *132*, 2116.
(43) Goodrich, B. F.; de la Fuente, J. C.; Gurkan, B. E.; Zadigian, D. J.; Price, E. A.; Huang, Y.; Brennecke, J. F. Experimental measurements of amine-functionalized anion-tethered ionic liquids with carbon dioxide. *Ind. Eng. Chem. Res.* **2011**, *50*, 111.
(44) Olafsson, P. G.; Bryan, A. M. Evaluation of thermal decomposition temperatures of amino acids by differential enthalpic analysis. *Microchim. Acta* **1970**, *5*, 871.
(45) Crank, J. *The Mathematics of Diffusion*, 2nd ed.; Oxford University Press: Oxford, 1975.
(46) Li, X. Y.; Hou, M. Q.; Zhang, Z. F.; Han, B. X.; Yang, G. Y.; Wang, X. L.; Zou, L. Z. Absorption of CO_2 by ionic liquid/polyethylene glycol mixture and the thermodynamic parameters. *Green Chem.* **2008**, *10*, 879.
(47) Zhang, F.; Fang, C. G.; Wu, Y. T.; Wang, Y. T.; Li, A. M.; Zhang, Z. B. Absorption of CO_2 in the aqueous solutions of functionalized ionic liquids and MDEA. *Chem. Eng. J* **2010**, *160*, 691.
(48) Zhao, W.; He, G. H.; Zhang, L. L.; Ju., J.; Dou, H.; Nie, F.; Li, C. N.; Liu, H. J. Effect of water in ionic liquid on the separation performance of supported ionic liquid membrane for CO_2/N_2. *J. Membr. Sci.* **2010**, *350*, 279.
(49) Ludwig, R.; Kragl, U. Do we understand the volatility of ionic liquids? *Angew. Chem., Int. Ed.* **2007**, *46*, 6582.
(50) Esperanca, J. M. S. S.; Lopes, J. N. C.; Tariq, M.; Santos, L. M. N. B. F.; Magee, J. W.; Rebelo, L. P. N. Volatility of aprotic ionic liquids - A review. *J. Chem. Eng. Data* **2010**, *55*, 3.
(51) Harper, N. D.; Nizio, K. D.; Hendsbee, A. D.; Masuda, J. D.; Robertson, K. N.; Murphy, L. J.; Johnson, M. B.; Pye, C. C.; Clyburne, J. A. C. Survey of carbon dioxide capture in phosphonium-based ionic liquids and end-capped polyethylene glycol using DETA (DETA = diethylenetriamine) as a model absorbent. *Ind. Eng. Chem. Res.* **2011**, *50*, 2822.